# Structure and dynamics of poly(1-naphthyl acrylate) in solution by 13C NMR spectroscopy

**ARTICLE** *in* MACROMOLECULES · MAY 1992

Impact Factor: 5.8 · DOI: 10.1021/ma00029a008



**2 AUTHORS:**

Apostolos Spyros
University of Crete
**50** PUBLICATIONS **863** CITATIONS
SEE PROFILE

Photis Dais
University of Crete
**125** PUBLICATIONS **2,192** CITATIONS
SEE PROFILE

# Structure and Dynamics of Poly(1-naphthyl acrylate) in Solution by $^{13}C$ NMR Spectroscopy

**A. Spyros and Photis Dais***

*Department of Chemistry, University of Crete, P.O. Box 1470, 711 10 Iraklion, Crete, Greece*

*Received April 9, 1991; Revised Manuscript Received August 22, 1991*

ABSTRACT: Carbon-13 spin–lattice relaxation times and NOE factors were measured as a function of temperature in two magnetic fields for poly(1-naphthyl acrylate) (PNA) in 1,1,2,2-tetrachloroethane-$d_2$. The relaxation data were interpreted in terms of chain segmental motion and naphthyl internal rotation by using the sharp cutoff model of Jones and Stockmayer (JS) and the Hall–Weber–Helfand (HWH) correlation function. Both models describe in a satisfactory and comparable manner the chain local motions of PNA resulting in approximately similar correlation times ($6 \times 10^{-9}$ s at 20 °C) and activation energy (19 kJ/mol) for cooperative segmental motions of the chain. Naphthyl internal rotation is described by a hindered rotation about the C(1)–O bond superimposed on segmental motions described by both models. They differ, however, in the time scale and angular amplitude of the naphthyl motion, which was found to be faster and less restricted with the JS description as compared to that using the HWH model, although both models give the same activation energy (ca. 13 kJ/mol) for the naphthyl rotation. Finally, the microtacticity of PNA is examined by $^{13}C$ NMR spectroscopy, and it is concluded that the stereochemistry of the propagation step conforms with Bernoullian statistics.

## Introduction

Measurements of $^{13}C$ nuclear magnetic relaxation parameters provide a powerful approach for elucidating the nature of local motions of polymer chains in solution. A number of models have been developed[1] for the interpretation of nuclear spin relaxation data. Among these, the three-bond jump model developed by Jones and Stockmayer[2] (JS) and that of Hall, Weber, and Helfand[3,4] (HWH) have proven to be successful in describing the polymer dynamics in solution. These models will be used to describe the segmental mobility of poly(1-naphthyl acrylate) (PNA) in 1,1,2,2-tetrachloroethane-$d_2$ (TCE) solvent. In addition to segmental mobility, the naphthyl internal rotation about the C(1)–O bond will be examined as well, using composite spectral densities based on the JS and HWH models, combined with the usual Woessner approach[5] for free rotation and the Gronski description[6] for restricted rotational diffusion.

The present study is extended to include the determination of the microstructure of PNA by employing $^{13}C$ NMR spectroscopy. PNA as well as other naphthyl-containing polymer systems is of interest, since they have been used[7,8] as model compounds to investigate photophysical processes, such as energy transfer between pendant naphthalene chromophores, that mimic similar effects in plant photosynthesis and have practical consequences in the photodegradation and/or photostabilization of commercial polymers.

## Experimental Section

PNA was synthesized by free-radical polymerization and purified according to the literature.[7] The molecular weight ($\bar{M}_w$) was determined by low-angle laser scattering using a KMX chromatic instrument and found to be $1.60 \times 10^5$.

$^{13}C$ NMR noise-decoupled spectra at 50 °C were obtained with a Varian XL-300 spectrometer operating at 75.4 MHz for the carbon nucleus. Instrument conditions were as follows: pulse angle, 45° (8 μs); repetition time, 2.0–2.5 s for sweep widths 15 000 Hz; 10 000–15 000 transients on 32K memory were accumulated for each experiment. Sweep widths of 1500–2000 Hz and repetition times of >8 s were used to achieve higher resolution for the $^{13}C{=}O$ resonance. Samples were 10% (w/v) in 1,1,2,2-tetrachloroethane-$d_2$. Chemical shifts were measured relative to the solvent peak and converted to δ(TMS) according to the relationship $\delta(\text{TMS}) = \delta((CDCl_2)_2) + 75.50$ ppm.

$^{13}C$ spin–lattice relaxation time experiments were conducted on Varian XL-200 (operating at 50.3 MHz for the carbon nucleus) and XL-300 spectrometers. The temperature was controlled to within ±0.1 °C by means of a precalibrated copper–constantan thermocouple in the probe insert. The relaxation times were measured by the standard inversion–recovery technique with a repetition time longer than $5T_1$. A total of 500–800 acquisitions were accumulated for each set of 11–13 "arrayed" $\tau$ values. Values of $T_1$ were determined by a three-parameter nonlinear procedure with a root-mean-square (rms) error of ±10% or better. $^{13}C$ NOE experiments were carried out by gated decoupling, at least three experiments being performed for each temperature value. Delays of at least 10 times the longest $T_1$ were used between 90° pulses. Samples of PNA in TCE were degassed by bubbling nitrogen gas for 2 min before use. Nevertheless, measurements with undegassed samples did not show any measurable change in the $T_1$ and NOE values relative to those of degassed samples.

Viscosity measurements were performed using an Ubbelohde type viscometer at 30 °C. The intrinsic viscosity and Huggins constant, $k'$, in eq 1 for PNA were found to be 0.1474 dL/g and 2.09, respectively.

$$\eta_{sp}/c = [\eta] + k'[\eta]^2 c \tag{1}$$

**Numerical Calculations.** The correlation times were calculated using the MOLDYN program[9] modified to include the various models used in the present study. To describe the segmental motion of the PNA chain employing the JS and HWH models, the $T_1$ and NOE values for the backbone CH group at both field strengths for a given temperature were used as input, and the best fit correlation times from each model were calculated using a Simplex routine to vary the parameters until the target function, $F$, defined in eq 2 as the sum of the squares of

$$F = \sum_{i=1}^{n} [(S_{i,\text{cal}} - S_{i,\text{exp}})/S_{i,\text{exp}}]^2$$

$$S = 1/T_1 \text{ and/or NOE} \tag{2}$$

the relative deviations between the experimental and calculated spin–lattice relaxation times $(T_1)_{exp}$ and $(T_1)_{cal}$, respectively, and/or NOE factors was a minimum. Values of the function $F$ on the order 0.01–0.001 were observed in the present calculations, reflecting a good fit. Relaxation parameters for the $CH_2$ group

0024-9297/92/2225-1062$03.00/0 

were not included in the minimization procedure. This resonance was broadened so much by the effects of tacticity that its relaxation parameters were difficult to measure accurately. The correlation times for naphthyl internal motion in JS and HWH models were subsequently determined for a given temperature by adjusting them to account for naphthyl relaxation data, while holding constant the parameters describing segmental chain motions at the values determined from the relaxation data of the backbone carbon.

## Results and Discussion

**Microstructure Determination.** Figure 1 illustrates the $^{13}C$ NMR spectrum of the PNA polymer. Peak assignments of the backbone carbons were made by analogy with the $^{13}C$ spectrum of poly(methyl acrylate)[10] and confirmed by correlations with the C–H multiplets in the off-resonance spectra. The carbonyl resonance was safely assigned as that appearing at the lowest fields. No attempt was made to assign the naphthyl carbons through 2D NMR experiments due to the very poorly resolved naphthyl proton resonances at 300 MHz. These carbons were assigned on the basis of model compounds,[11] i.e., 1-acetoxy-1-hydroxymethyl and 1-carbomethoxynaphthalenes, and verified by $^{13}C$ $T_1$ measurements. These arrangements are listed in Table I. Note that carbons C-6 and C-8a are overlapped. This overlap persists up to about 70 °C. Beyond that temperature the C-8a peak shifts to higher fields and finally overlaps with the peak of carbon C-7. Therefore, in the subsequent relaxation experiments only the $T_1$'s for the C-6 or the C-7 carbons can be measured.

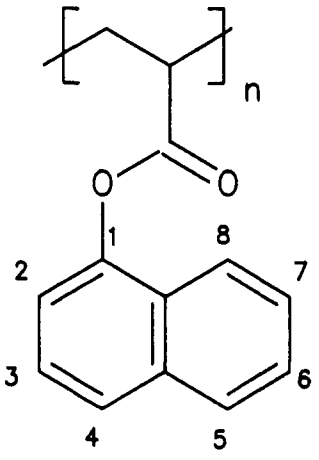


Figure 1 shows that several carbons in the PNA spectrum are stereoselective. In particular, the signals corresponding to the CH backbone carbon and the carbonyl carbon are split into three and four lines, respectively. The splitting pattern for these resonances is shown in Figure 1 in an expanded form. Relative intensities are given in Table I. Assignment is based on triad probabilities and the assumption that PNA fits Bernoullian statistics.[12] The proposed assignments in Table I are in keeping with those reported for poly(methyl acrylate).[10] The distribution of the relative intensities fits a Bernoullian propagation model with $P_m = 0.40$. Number-average sequence lengths for meso and racemic additions are 1.7 and 2.6, respectively.

The splitting of the methylene signal (Figure 1) can be assigned to mixed diad and tetrad stereosequences, in analogy to what has been suggested by several authors for poly(methyl acrylate).[13] In the present study the various components of the $^{13}CH_2$ peak are not resolved well enough to guarantee a valid analysis of higher order sequences.

**Table I**
**$^{13}C$ Chemical Shifts and Experimental and Calculated Microtacticities for PNA in TCE Solution**

| carbon | δ, ppm | assignments | intensity exptl | intensity calcd[b] |
|---|---|---|---|---|
| | 175.28 | mrrm | 0.08 | 0.08 |
| C=O | 174.94 | rrrm + rrrr | 0.29 | 0.30 |
| | 174.57 | mr | 0.47 | 0.48 |
| | 174.18 | mm | 0.16 | 0.16 |
| | 43.83 | rr | 0.36 | |
| CH | 43.65 | mr | 0.49 | |
| | 43.35 | mm | 0.15 | |
| | 38.81 | r | 0.59 | 0.60 |
| $CH_2$ | 37.32 | m | 0.41 | 0.40 |
| C-1 | 147.74 | | | |
| C-2 | 119.69 | | | |
| C-3 | 126.79 | | | |
| C-4 | 127.67 | | | |
| C-5 | 129.33 | | | |
| C-6[a] | 128.31 | | | |
| C-7 | 128.02 | | | |
| C-8 | 122.37 | | | |
| C-4a | 135.96 | | | |
| C-8a[a] | 128.31 | | | |

[a] Overlapped peaks (see text). [b] Assuming Bernoullian statistics ($P_m = 0.40$).

**Table II**
**Carbon-13 Spin–Lattice Relaxation Times ($T_1$, in ms) and NOE Factors[a] of Protonated Carbons[b] of PNA in TCE-$d_2$**

| | backbone carbon | | C-2, C-3, C-6, C-7[c] | | C-4, C-5, C-8[c] | |
|---|---|---|---|---|---|---|
| t, °C | 50 MHz | 75 MHz | 50 MHz | 75 MHz | 50 MHz | 75 MHz |
| 20 | 150 (1.37) | 257 (1.26) | 147 (1.53) | 215 (1.44) | 148 (1.34) | 241 (1.25) |
| 40 | 125 (1.53) | 205 (1.44) | 146 (1.69) | 205 (1.43) | 137 (1.50) | 206 (1.29) |
| 60 | 114 (1.53) | 175 (1.46) | 160 (1.83) | 218 (1.60) | 132 (1.66) | 187 (1.40) |
| 80 | 104 (1.63) | 165 (1.53) | 184 (2.09) | 249 (1.85) | 137 (1.77) | 188 (1.55) |
| 100 | 109 (1.85) | 171 (1.60) | 213 (2.37) | 300 (2.11) | 146 (1.99) | 198 (1.67) |
| 120 | 114 (2.05) | 173 (1.76) | 247 (2.57) | 367 (2.25) | 153 (2.14) | 221 (1.84) |

[a] Values in parentheses. [b] $CH_2$ carbon is not included (see text). [c] The difference of $T_1$ and NOE from each type of carbon of the naphthyl ring is within ±5%, so that average values are reported.

However, the observed diads of this resonance (Figure 1) conform with the Bernoullian propagation model.

**Dynamics of PNA.** Table II summarizes the $^{13}C$ $T_1$ values and NOE factors for the methine backbone carbon and the protonated naphthyl carbons of PNA as a function of temperature in two magnetic fields. As can be seen, the $T_1$ values of the backbone carbon reach a minimum in both fields as the temperature increases and they increase with increasing magnetic field. This indicates that the motion of the PNA chain is in the regime of long correlation times outside the extreme narrowing condition, reaching a minimum at ca. 80 °C. This feature of the $T_1$ values, and the fact that the NOE factors are invariably below the extreme narrowing limit in the whole range studied for both fields, indicates that a single-exponential correlation function, i.e., isotropic motion, is inadequate to account for these relaxation data. Indeed, the relaxation time at the minimum is at both fields approximately twice as long as expected from the single-correlation time theory.

The relaxation times of the C-2, C-3, C-6, or C-7 carbons of the naphthyl moiety on the one hand and the relaxation times of the C-4, C-5, and C-8 carbons on the other hand are all similar within experimental error at 20 and 40 °C

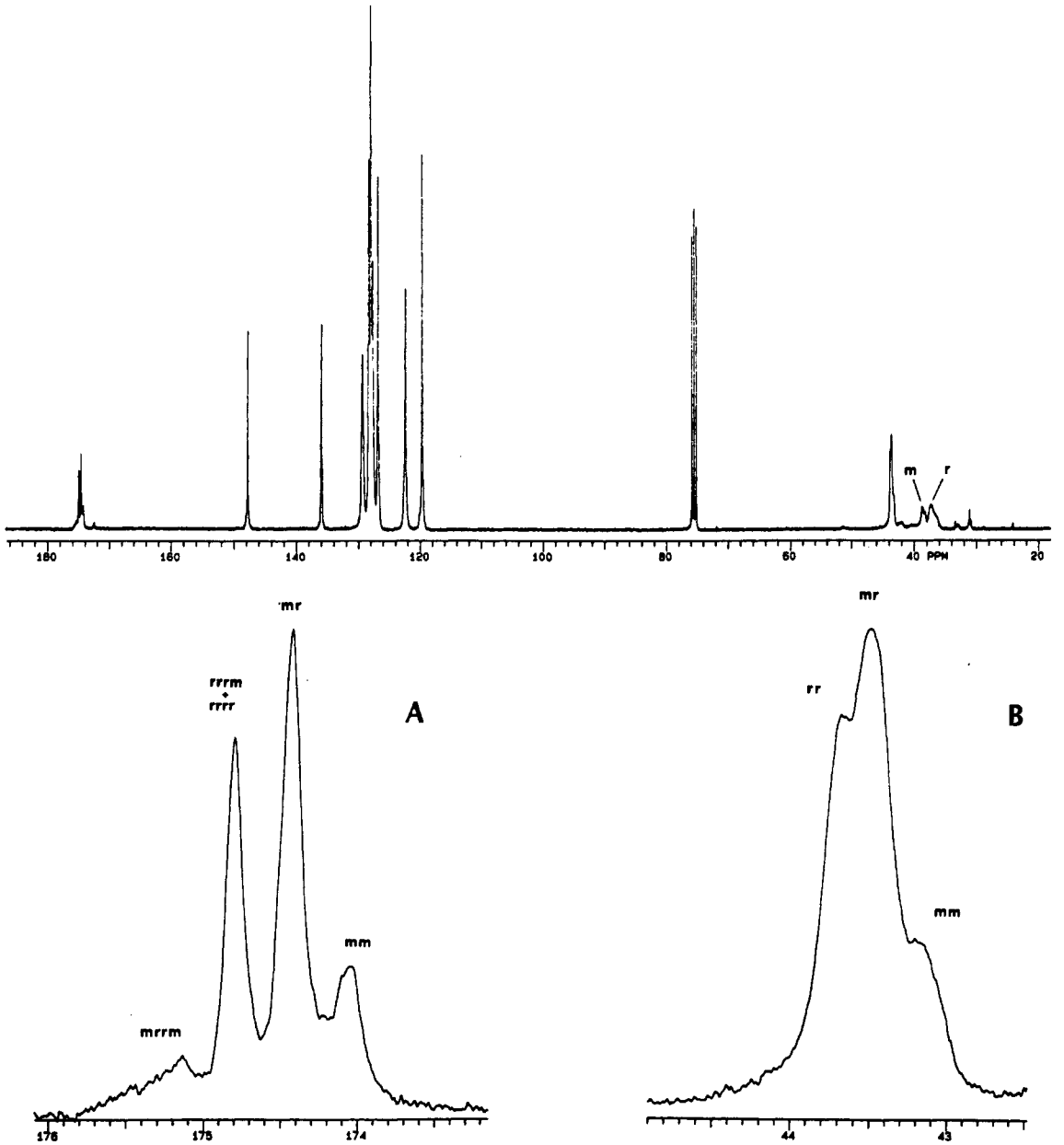


**Figure 1.** Proton-decoupled $^{13}C$ spectrum of poly(1-naphthyl acrylate). A and B show details of the tacticity for the carbonyl and methine resonances, respectively.

(Table II), whereas at higher temperatures the relaxation times of the former group of carbons become higher than those of the latter group. Moreover, the relaxation parameters in each group are similar within 5–10%, so that an average value of the relaxation parameters is considered for the present analysis and shown in Table II. These observations indicate that the rate of the naphthyl internal motion about the C(1)–O bond is slow at low temperature and it becomes comparable or faster than the rate of the chain segmental motion as the temperature increases. This expectation is a consequence of the different orientations of the internuclear vectors relative to the C(1)–O axis for the two types of position. A $^{13}C$–$^{1}H$ vector parallel to the C(1)–O axis will be little affected by internal rotation about that axis, whereas internuclear vectors making an angle of about 60° with the C(1)–O axis are expected to be influenced by internal rotation.[14]

However, it should be noted that additional flexibility about the CH–CO bond of the ester group (rotation about the OC–O bond is expected to be very slow owing to significant conjugation effects[15]) is expected to affect the rate of the naphthyl motion. The effectiveness of this additional motion is better reflected on the relaxation times of the C-4, C-5, and C-8 carbons at higher temperatures, which are longer than those of the backbone CH carbon (Table II). Unfortunately, the additional mode of reorientation is not amenable to an effective analysis with insufficient relaxation data. Therefore, only an apparent relaxation rate and activation energy can be estimated for the naphthyl internal motion of PNA from the present experimental data.

Modeling the dynamics of PNA, three general types of motion are considered: (1) the overall tumbling motion, (2) segmental backbone rearrangement, and (3) internal motion relative to the backbone units. Each of these motions is considered as an independent source of motional modulation of the dipole–dipole interaction so that the composite autocorrelation function is a product of the correlation functions associated with each motion. For sufficiently high molecular weight polymers the overall motion is much slower than the chain local motions, thus being a negligible contributor to the relaxation of the backbone carbons.

Table III
Simulation Parameters for PNA Using JS and HWH Models

| | | JS | | | HWH | | | |
|---|---|---|---|---|---|---|---|---|
| $t$, °C | $2m-1$ | $10^{-9}\tau_h$, s | $10^{-10}\tau_{ir}$, s | $l°$ | $10^{-8}\tau_0$, s | $10^{-9}\tau_1$, s | $10^{-10}\tau_{lr}$, s | $l°$ |
| 20 | 5 | 6.05 | | | [a] | 6.10 | | |
| 40 | 5 | 3.61 | | | | 3.66 | | |
| 60 | 5 | 2.02 | 0.078 | 162 | 5.58 | 1.99 | 0.54 | 100 |
| 80 | 5 | 1.42 | 0.059 | 172 | 1.53 | 1.50 | 0.40 | 129 |
| 100 | 9 | 1.23 | 0.047 | 246 | 1.03 | 1.20 | 0.33 | 159 |
| 120 | 9 | 0.86 | 0.039 | 259 | 0.60 | 0.84 | 0.26 | 173 |
| $E_a$, kJ/mol | | 18.5 | 12.5 | | 39 | 19 | 13 | |
| $10^{12}\tau$, s | | 3.0 | 0.85 | | 0.04 | 2.61 | 0.54 | |
| concn coeff | | 0.993 | 0.998 | | 0.972 | 0.994 | 0.998 | |

[a] The simulation parameter $\tau_0$ for the HWH model is undetermined, ranging between $10^{-6}$ and $10^{-8}$ s in the fitting procedure.

The correlation time of the overall rotary diffusion, $\tau_R$, was estimated at infinite dilution as a function of the molecular weight, $M$, and the intrinsic viscosity, $[\eta]$, of the polymer solution in a given solvent of viscosity, $\eta_0$, through the hydrodynamic equation

$$\tau_R = 2M[\eta]\eta_0/3RT \tag{3}$$

and was found to be $0.9 \times 10^{-6}$ s at 30 °C. This value changes only slightly, considering a solution of finite concentration (10% w/v) and the effect of the molecular weight distribution of PNA sample.[16] This long correlation time guarantees the preponderance of the local motions as the major relaxation source for the protonated carbons of PNA.

The second type of motion, i.e., backbone rearrangement, will be described by the JS model, in which the motion is modeled as a three-bond jump on a tetrahedral lattice, i.e., as a "crankshaft" motion. The time scale of the segmental motion is described by a harmonic mean-correlation time, $\tau_h$, and the breadth of the distribution of correlation times is characterized by the number of bonds, $m$, involved in the cooperative motion or the quantity, $2m-1$, which stands for the chain segment expressed in bonds that are coupled to the central bonds. The JS spectral density is

$$J_i(\omega_i) = 2\sum_{k=1}^{s} G_k \frac{\tau_{k0}}{1+\omega_i^2\tau_{k0}^2}$$

$$\tau_{k0}^{-1} = \tau_k^{-1} + \tau_R^{-1}$$

$$\tau_k^{-1} = w\lambda_k \qquad s = (m+1)/2$$

$$\lambda_k = 4\sin^2[(2k-1)\pi/2(m+1)]$$

$$\tau_h^{-1} = 2w \qquad \gamma = \ln 9$$

$$G_k = 1/s + (2/s)\sum_{q=1}^{s-1}\exp(-\gamma q)\cos[(2k-1)\pi q/2s] \tag{4}$$

where $w$ is the rate of occurrence of the three-bond jump of the polymer backbone usually expressed as the harmonic mean-correlation time, $\tau_h^{-1} = 2w$.

The second theoretical model for conformational dynamics developed by Hall, Weber, and Helfand takes into account correlated pair transitions and isolated transitions occurring with correlation times $\tau_1$ and $\tau_0$, respectively. The pair transitions ensure the propagation along the chain, while isolated, i.e., single-bond, transitions are responsible for the damping. The HWH spectral density is

$$J_i(\omega_i) = 2\{[(\tau_0^{-1})(\tau_{01}^{-1} + \tau_1^{-1}) - \omega_i^2]^2 + (2\tau_{01}^{-1}\omega_i)^2\}^{-1/4} \times \cos[1/2 \arctan\{2\tau_{01}^{-1}\omega_i/[\tau_0^{-1}(\tau_{01}^{-1} + \tau_1^{-1}) - \omega_i^2]\}]$$

$$\tau_{01}^{-1} = \tau_0^{-1} + \tau_1^{-1} \tag{5}$$

It is worth mentioning that the above expression for the spectral density was originally derived by Fourier transformation of a conformational correlation function. Nevertheless, this correlation function has proven to fit well both the orientational and conformational decay curves obtained from experiments and Brownian simulations. In addition, the recent study by Lin et al.,[17] which shows a connection between the JS and HWH spectral densities, supports the use of the latter to describe backbone motions in polymer systems.

Assuming purely $^{13}C$–$^1H$ dipolar relaxation, the spin–lattice relaxation time and NOE factors can then be calculated from the following well-known equations from the above expressions for $J_i(\omega_i)$

$$1/T_1 = \frac{\hbar^2\gamma_C^2\gamma_H^2}{10r_{CH}^6}[J_0(\omega_H - \omega_C) + 3J_1(\omega_C) + 6J_2(\omega_H + \omega_C)] \tag{6}$$

$$\mathrm{NOE} = 1 + \frac{\gamma_H}{\gamma_C}\left[\frac{6J_2(\omega_H - \omega_C) - J_0(\omega_H - \omega_C)}{J_0(\omega_H - \omega_C) + 3J_1(\omega_C) + 6J_2(\omega_H + \omega_C)}\right] \tag{7}$$

The interpretation of the relaxation data on the basis of eqs 6 and 7 requires one to fix or determine the C–H bond distance. No experimental value for the backbone C–H bond length of PNA exists in the literature nor for the related PMA and PMMA polymers. A value of 1.11 Å for the backbone C–H distance offered the best quality of the fitting and reasonable simulation parameters for both models. A value of 1.09 Å was taken for the naphthyl C–H bond length.

The best fit of the $T_1$ data is summarized in Table IV, whereas the simulation parameters of the JS and HWH models are tabulated in Table III. The reproduced values are within 10% of the experimental values or within experimental error.

A salient feature of the simulation parameters is that $\tau_h$ and $\tau_1$, the correlation times for cooperative segmental motions in the two models, are comparable. This is quite apparent in the Arrhenius parameters in Table III, where both activation energies and prefactors are similar for $\tau_h$ and $\tau_1$. The similarity between $\tau_h$ and $\tau_1$ has been rationalized[18] on the basis that both models derive correlation functions for cooperative local motions in terms

of conformational diffusion, although these models were developed from quite different starting points.

The extent of coupling as measured by $2m - 1$ indicates a rather narrow distribution of correlation times involving three to five bonds in the crankshaft motion. However, this parameter plays a secondary role[17,18] in the simulation of the three-bond jump model, and its value is more useful as an indicator of degrees of freedom available in the polymer chain. Recently, a modification of the HWH model was introduced by Dejean de la Batie, Laupretre, and Monnerie[19] by considering an additional independent motion superimposed on the backbone rearrangement as described by the HWH model. This motion, which must be faster and thus more local than the orientation diffusion process along the chain, has been attributed to molecular librations of a limited extent of the C–H vectors inside a cone of half-angle $\theta$, the axis of which is the rest position of the C–H bond. This model has been successfully applied to several polymer systems[19–21] in solution, leading to the interesting conclusion that different carbon sites in the polymer backbone may not experience exactly the same local dynamics. However, application of this model to PNA failed to reproduce the experimental $T_1$ values at the minimum (115 ms (50.3 MHz), 174 ms (75.4 MHz) at 80 °C). This observation may reflect a high steric hindrance to the librational motion of the corresponding C–H vector due to the presence of the adjacent bulky naphthyl group. Internal motions, such as naphthyl internal rotation, are added as independent motions, in the form of an appropriate correlation function describing either a diffusional stochastic process or jumps among energy minima in the potential energy curve. Composite spectral densities for the JS and HWH models describing phenyl internal rotation superimposed on chain segmental motions have been derived[22,23] and applied successfully in the interpretation of the nuclear magnetic and dielectric relaxation data on polystyrene.[23] Attempts to interpret the relaxation data of the naphthyl group in PNA using either a stochastic diffusion process or jumps in a 2-fold potential barrier were unsuccessful. Therefore, a restricted rotation model developed by Gronski[6] has been adopted to describe the naphthyl internal rotation in PNA. The composite spectral density for the JS model is[24]

$$J_i(\omega_i) = 2\sum_{k=1}^{s} G_k \frac{A\tau_{k0}}{1+\omega_i^2\tau_{k0}^2} + \frac{B}{l^2}\left\{[(1-\cos l)^2+\sin^2 l]\frac{\tau_{k0}}{1+\omega_i^2\tau_{k0}^2} + \frac{1}{2}\sum_{n=1}^{\infty}\left[\left\{\frac{[1-\cos(l-n\pi)]}{(1-n\pi/l)}+\frac{[1-\cos(l+n\pi)]}{(1+n\pi/l)}\right\}^2 + \left\{\frac{\sin(l-n\pi)}{(1-n\pi/l)}+\frac{\sin(l+n\pi)}{(1+n\pi/l)}\right\}^2\right]\frac{\tau_{nk0}}{1+\omega_i^2\tau_{nk0}^2}\right\} + \frac{C}{2l^2}\left\{\frac{1}{2}[(1-\cos 2l)^2+\sin^2 2l]\frac{\tau_{k0}}{1+\omega_i^2\tau_{k0}^2} + \sum_{n=1}^{\infty}\left[\left\{\frac{[1-\cos(2l-n\pi)]}{(2-n\pi/l)}+\frac{[1-\cos(2l+n\pi)]}{(2+n\pi/l)}\right\}^2 + \left\{\frac{\sin(2l-n\pi)}{(2-n\pi/l)}+\frac{\sin(2l+n\pi)}{(2+n\pi/l)}\right\}^2\right]\frac{\tau_{nk0}}{1+\omega_i^2\tau_{nk0}^2}\right\} \quad (8)$$

where

$$\tau_{nk0}^{-1} = \tau_k^{-1} + \lambda_n$$

$$\tau_{k0}^{-1} = \tau_k^{-1} + \tau_R^{-1}$$

$$\lambda_n = (n\pi/l)^2 D_{ir}$$

and

$$A = (3\cos^2\Delta - 1)^2/4$$

$$B = 3(\sin^2 2\Delta)/4$$

$$C = 3(\sin^4\Delta)/4$$

$D_{ir}$ is the diffusion constant for the naphthyl rotation, $\Delta$ is the angle between the internuclear C–H vector and the C(1)–O axis of rotation, and $l$ is the amplitude of the restricted motion.

The HWH description of segmental motion can also be combined with restricted anisotropic diffusion[24]

$$J_i(\omega_i) = AJ_i^{01}(\omega_i) + \frac{B}{l^2}\left\{[(1-\cos l)^2+\sin^2 l]J_i^{01}(\omega_i) + \frac{1}{2}\sum_{n=1}^{\infty}\left[\left\{\frac{[1-\cos(l-n\pi)]}{(1-n\pi/l)}+\frac{[1-\cos(l+n\pi)]}{(1+n\pi/l)}\right\}^2 + \left\{\frac{\sin(l-n\pi)}{(1-n\pi/l)}+\frac{\sin(l+n\pi)}{(1+n\pi/l)}\right\}^2\right]J_i^{\lambda n}(\omega_i)\right\} + \frac{C}{2l^2}\left\{\frac{1}{2}[(1-\cos 2l)^2+\sin^2 2l]J_i^{01}(\omega_i) + \sum_{n=1}^{\infty}\left[\left\{\frac{[1-\cos(2l-n\pi)]}{(2-n\pi/l)}+\frac{[1-\cos(2l+n\pi)]}{(2+n\pi/l)}\right\}^2 + \left\{\frac{\sin(2l-n\pi)}{(2-n\pi/l)}+\frac{\sin(2l+n\pi)}{(2+n\pi/l)}\right\}^2\right]J_i^{\lambda n}(\omega_i)\right\} \quad (9)$$

where $J_i^{01}(\omega_i)$, $\tau_{01}$, $\lambda_n$, and $D_{ir}$ are defined in eqs 5 and 8

$$J_i^{\lambda n}(\omega_i) = \{[(\tau_0^{-1}+\lambda_n)(\tau_{01}^{-1} + \tau_1^{-1}+\lambda_n) - \omega_i^2]^2\}^{-1/4}\cos\{1/2\arctan[2(\tau_{01}^{-1}+\lambda_n)\omega_i/[(\tau_0^{-1}+\lambda_n)(\tau_{01}^{-1}+\lambda_n) - \omega_i^2]]\} \quad (10)$$

The simulation parameters for anisotropic rotation are displayed in Table III for the case where segmental motion is characterized with the JS and the HWH models on the basis of the CH backbone carbon data. Table IV depicts the best fit of the average $T_1$ and NOE values of the C-2, C-3, C-6, or C-7 carbons. Agreement between experimental and calculated values is very good. Also, very good agreement was obtained for the NOE factors.

The naphthyl internal motion as described by the model of restricted diffusion ($\tau_{ir} = 1/6D_{ir}$, values in Table III) is faster than the backbone rearrangement described by both JS and HWH models ($\tau_h$ and $\tau_1$ values). The fast internal motion is also reflected on the simulated values of the angular amplitude which increase with temperature toward the free rotation limit. However, mention should be made on the fact that these simulated values as well as the calculated activation energy of ca. 13 kJ/mol for the naphthyl motion are affected by a second rotation about the CH–CO bond. At higher temperatures populations arising from rotations about this internal axis are expected to

**Table IV**
**Simulated Relaxation Parameters $T_1$ (in ms) and NOE Factors[a] for PNA**

| | backbone carbon | | | | C-2, C-3, C-6, or C-7 | | | |
|---|---|---|---|---|---|---|---|---|
| | 50 MHz | | 75 MHz | | 50 MHz | | 75 MHz | |
| $t$, °C | JS | HWH | JS | HWH | JS | HWH | JS | HWH |
| 20 | 142 (1.24) | 142 (1.23) | 262 (1.20) | 264 (1.19) | | | | |
| 40 | 123 (1.35) | 123 (1.35) | 205 (1.26) | 205 (1.25) | | | | |
| 60 | 111 (1.54) | 114 (1.57) | 178 (1.40) | 174 (1.41) | 152 (1.71) | 155 (1.73) | 228 (1.69) | 224 (1.66) |
| 80 | 106 (1.65) | 110 (1.70) | 168 (1.51) | 164 (1.52) | 184 (1.80) | 184 (1.96) | 244 (1.76) | 249 (1.92) |
| 100 | 112 (1.81) | 111 (1.83) | 179 (1.61) | 162 (1.63) | 222 (2.18) | 223 (2.18) | 286 (2.17) | 284 (2.17) |
| 120 | 123 (1.92) | 117 (1.96) | 181 (1.78) | 164 (1.79) | 265 (2.29) | 267 (2.31) | 335 (2.31) | 331 (2.29) |

[a] Values in parentheses.

become larger, allowing an increase of conformational changes other than those occurring because of the rotation about the C(1)–O bond. This would result in a more effective rotational averaging from 60 to 120 °C. Although the rate of the rotation about the CH–CO bond cannot be determined as mentioned earlier, the calculated $\tau_{ir}$ values suggest a rather fast, but restricted, naphthyl internal rotation from 60 °C to higher temperatures. This restricted motion may be attributed to collisions among neighboring naphthyl groups. Since this radically polymerized atactic PNA is rich in syndiotacticity, collisions among next neighboring naphthyl chromophores cannot be excluded.

One aspect of the interpretation which is not very satisfying is that the correlation times, $\tau_{ir}$, are of about an order longer for the HWH model than those for the JS model. Also, the faster motion as described by the JS model is accompanied by a larger angular amplitude than that of the HWH model, reflecting a less hindered motion for the former model.

At this time, the physical significance of such a behavior of the naphthyl motion upon changing the description of segmental motion is not clear, and it may also be only an artifact of the interpretation, since the HWH model was derived on a very local molecular basis, considering conformational jumps on a polymethylene chain without pendant groups.[25] It should be noted that, in a similar study[18] on poly($\beta$-hydroxy butyrate), the $\tau_{ir}$ values for the methyl internal rotation were found longer for the HWH model than those for the JS description. However, for a thorough understanding of the present experimental results, and particularly those concerned with the amplitude of the restricted internal motion, calculations should be performed to analyze the conformational characteristics of PNA. These molecular modeling studies are currently in progress.

**Acknowledgment.** Financial support from the University of Crete is appreciated. This work was also supported by NATO Grant CRG910406.

## References and Notes

(1) Heatley, F. *Prog. Nucl. Magn. Reson. Spectrosc.* **1979**, *13*, 47. Schaefer, J. *Top. Carbon-13 NMR Spectrosc.* **1974**, *1*, 150.
(2) Jones, A. A.; Stockmayer, W. H. *J. Polym. Sci., Polym. Phys. Ed.* **1977**, *15*, 847.
(3) Hall, C. K.; Helfand, E. *J. Chem. Phys.* **1982**, *77*, 3275.
(4) Weber, T. A.; Helfand, E. *J. Phys. Chem.* **1983**, *87*, 2881.
(5) Woessner, D. E.; Snowden, B. S.; Meyer, G. H. *J. Chem. Phys.* **1969**, *50*, 719.
(6) Gronski, W. *Makromol. Chem.* **1979**, *180*, 1119.
(7) Aspler, J. S.; Guillet, J. E. *Macromolecules* **1979**, *12*, 1082.
(8) Holden, D. A.; Guillet, J. E. *Developments in Polymer Photochemistry*; Allen, N. S., Ed.; Applied Science Publishers: Barking, Essex, U.K., 1980.
(9) Craik, D. J.; Kumar, A.; Levy, G. C. *J. Chem. Inf. Comput. Sci.* **1983**, *1*, 30.
(10) Matsuzaki, K.; Kanai, T.; Kawamura, T.; Matsumoto, S.; Uryu, T. *J. Polym. Sci., Polym. Chem. Ed.* **1973**, *11*, 961.
(11) Hansen, P. E. *Org. Magn. Reson.* **1979**, *12*, 109.
(12) Bovey, F. A. *High Resolution NMR of Macromolecules*; Academic Press: New York, 1972; Chapters III and VIII.
(13) Randall, J. C. *Polymer Sequence Determination: Carbon-13 NMR Methods*; Academic Press: New York, 1977.
(14) Levy, G. C.; White, D. M.; Anet, F. A. *J. Magn. Reson.* **1972**, *6*, 453. Dais, P. *Magn. Reson. Chem.* **1987**, *25*, 141.
(15) Henrichs, P. M.; Hewitt, J. M.; Russel, G. A.; Sandhu, M. A.; Grashof, M. R. *Macromolecules* **1981**, *14*, 1770.
(16) Dais, P. *Carbohydr. Res.* **1987**, *169*, 73.
(17) Lin, Y. Y.; Jones, A. A.; Stockmayer, W. H. *J. Polym. Sci., Polym. Phys. Ed.* **1984**, *22*, 2195.
(18) Dais, P.; Nedea, M. E.; Morin, F. G.; Marchessault, R. H. *Macromolecules* **1989**, *22*, 4208.
(19) Dejean de la Batie, R.; Laupretre, F.; Monnerie, L. *Macromolecules* **1988**, *21*, 2045.
(20) Dejean de la Batie, R.; Laupretre, F.; Monnerie, L. *Macromolecules* **1988**, *21*, 5052; **1989**, *22*, 122.
(21) Dais, P.; Nedea, M. E.; Morin, F. G.; Marchessault, R. H. *Macromolecules* **1990**, *23*, 3387.
(22) Connoly, J. J.; Gordon, E.; Jones, A. A. *Macromolecules* **1984**, *17*, 722.
(23) Jones, A. A. *J. Polym. Sci., Polym. Phys. Ed.* **1977**, *15*, 863.
(24) Tarpey, M. F.; Lin, Y. Y.; Jones, A. A.; Inglefield, P. T. *ACS Symp. Ser.* **1984**, *247*, 67.
(25) Viovy, J. L.; Monnerie, L.; Brochon, J. C. *Macromolecules* **1983**, *16*, 1845.

**Registry No.** PNA (homopolymer), 28156-44-7.